Materials Research Proceedings 41 (2024) 449-456 https://doi.org/10.21741/9781644903131-50

A solid-beam approach for mesoscopic analysis of textile reinforcements forming simulation

LACROIX Baptiste[1,a *], COLMARS Julien[1,b], PLATZER Auriane[1,c], NAOUAR Naim[1,d], VIDAL-SALLÉ Emmanuelle[1,e], BOISSE Philippe[1]

[1]Université de Lyon, INSA-Lyon, LaMCoS UMR5259, F-69621, France

[a]baptiste.lacroix@insa-lyon.fr, [b]julien.colmars@insa-lyon.fr, [c]auriane.platzer@insa-lyon.fr
[d]naim.naouar@insa-lyon.fr, [e]emmanuelle.vidal-salle@insa-lyon.fr

Keywords: Meso-Scale Model, Solid-Beam, Fibrous Element, Hyperelastic

Abstract. Draping and forming of textile reinforcements are usually performed thanks to finite element models with continuous media assumption. The specific purpose of mesoscale model is to faithfully reproduces defects like yarn buckling or gapping during the process. Such defects are crucial outputs because they have huge impacts on mechanical and permeability properties of the whole textile. However, mesoscopic analysis usually leads to expensive computation cost and needs to be optimized to propose a cost-effective response to this problem. Thus, this document aims to develop a solid-beam approach for mesoscale model, with coarse geometric assumption but with finite element and constitutive law formulation taking into account the fibrous aspect of the fabric.

Introduction

The principle of mesoscopic analysis is to consider each yarn of a reinforcement as a continuous medium which mimics the geometric description of the fabric, as for example, its weaving pattern. Thanks to periodicity, textile studies can be reduced to a representative volume element (RVE), or unit-cell. The RVE can be either modelled from CAD software or deduced from micro-computed tomography (μCT) which enables to access to characteristics within the textile [1, 2]. It can be especially useful when yarn cross section shape and contact areas are critical inputs of the simulation. Such models are commonly meshed with isoparametric hexahedral elements associated with transverse isotropic 3D constitutive laws, either hypoelastic [2, 3] or hyperelastic [4]. Typically, mesoscopic RVE analysis can be relevant to simulate characterization test of woven fabrics [5].

When the purpose consists in modelling the entire textile, macroscopic scale is often chosen because of its efficiency. It can predict defects such as wrinkling [6, 7] but mesoscale models are necessary to highlight yarn buckling or gaping. However, very detailed and rich modelling might not be the most accurate because of their high computational costs (about one week of computation in case of forming simulation). To tackle this problem, some mixed meso-macro models have been proposed to give local mesoscopic analysis on macroscopic model. These works were mostly focused on 2D and 3D woven fabrics forming processes [8, 9].

Some assumptions can be made to simplify models and get more efficient computation with full mesoscopic analysis [10], but these models must be optimized to improve kinematic fidelity regarding experimental results.

To properly model the behaviour of textiles, classical Cauchy mechanics is not relevant, as has been experimentally highlighted [11]. Indeed, since fibrous media kinematics is guided by quasi-inextensibility of fibres and their relative sliding, tension and bending stiffness must be independent [12, 13]. These considerations motivated the development of a new finite element formulation which include the fibrous aspect [14, 15], which has mainly been used for macroscopic analysis so far.

Materials Research Proceedings 41 (2024) 449-456 https://doi.org/10.21741/9781644903131-50

In the present work, the formulation is extended to mesoscopic scale by modelling yarns as fibrous beams with deformable cross section. A new fibrous solid-beam element is developed for this purpose.

Bending behaviour

In order to ensure independence between tension and bending behaviour, a specific kinematic-based method called neighbour element method (NEM) is used. It has been initially developed for stamping simulation of metal sheets [16], to calculate curvature of shell element, for out-of-plane bending, without using rotational degrees of freedom (DOF). The principle holds in the fact that rotations can be directly expressed though out-of-plane displacement of neighbouring elements nodes. In addition, specific boundary conditions must be defined when an has no neighbour, as proposed in [17, 18].

To calculate their curvature, fibres are considered as Bernoulli beams (see Fig.1), which means that their curvature is linear along their neutral axis and can be entirely determined by the cross-section rotation of each side (see θ_i in Fig.1). In the case of a 2D problem, the NEM is represented in Fig. 2 and can be summarize as follows.

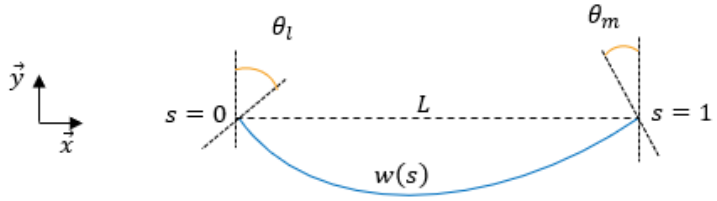

Fig.1°: Scheme of the parametric curve of the neutral axis of a Bernoulli beam.

For each beam of the model, its relative rotation with respect to its neighbour, (see α_i in Fig.2) is known from the initial undeformed configuration. The rotation angle can be calculated thanks to the projection of the nodal displacement in the normal direction. Moreover, the two circular arcs interpolating either the three nodes on the left (k, l, m) (red curve on Fig.2) or the three nodes on the right (l, m, p) (green curve on Fig.2) enable to calculate the cross-section orientation with relative rotation angles.

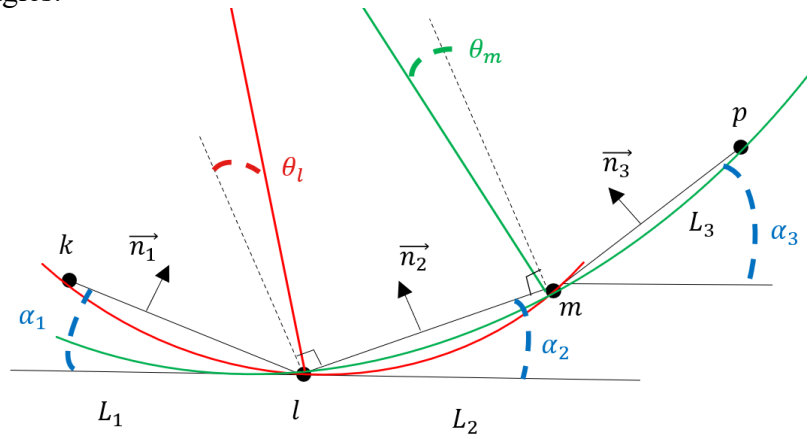

Fig.2°: Illustration of the NEM for one beam element in 2D

Each increment of relative rotation α_i can be calculated with the incremental nodal displacement. As an example, this would be the formula for the kl two node Bernoulli beam represented in Fig.2:

$$\delta\alpha_1 = \frac{1}{L}(\boldsymbol{n_1} \cdot \boldsymbol{\delta u_l} - \boldsymbol{n_1} \cdot \boldsymbol{\delta u_m}) \quad (1)$$

with $\boldsymbol{n_1}$ the unitary vector normal to the neutral axis elements, $\boldsymbol{\delta u_l}$ and $\boldsymbol{\delta u_m}$ the nodal incremental displacement of nodes k and l respectively.

The proposed NEM is implemented in an explicit dynamic framework [19]. Summing over the increments for large displacement simulation, the integrated curvature χ of the element lm then writes:

$$\chi(s) = \frac{\partial^2 N_l}{\partial x^2}\theta_l + \frac{\partial^2 N_m}{\partial x^2}\theta_m \tag{2}$$

where $s \in [0;1]$ is the local coordinate of the beam element in its reference configuration (see Fig.1), N_l and N_m are the shape function associated to the bending mode, defined by:

$$N_l(s) = L_2(s^3 - s^2)\ ;\ N_m(s) = L_2(s^3 - 2s^2 + s) \tag{3}$$

with L_2 the length of the element of interest lm (see Fig.2). Then, the cross-section rotations at the nodes k and l are obtained by:

$$\theta_l = \frac{-L_2}{L_2+L_1}(\alpha_1 + \alpha_2)\ ;\ \theta_m = \frac{L_2}{L_2+L_3}(\alpha_3 - \alpha_2) \tag{4}$$

For a 3D formulation of the NEM, we assume that the curvature can be represented by a first order tensor whose components are deduced from the 2D formulation in two orthogonal planes containing the fibre direction.

As for the material response, even if irreversible phenomena occur when a yarn is bent cyclically [20], elastic behaviour is sufficient to simulate textile forming process [21]. The present work thus assumes isotropic linear elastic bending behaviour, which has shown quite convincing results in previous fibrous element studies [14,15].

Behaviour of the yarn

A yarn can be composed of thousands of more or less aligned fibres which are mostly free to rearrange and slide between each other. Consequently, the fibre direction is a preferential one and can be used to describe the material behaviour. It implies that a transverse isotropic law should be applied. Moreover, it has been stated that the fibre density does not evolve in the section orthogonal to the fibre direction [22]. As a consequence, the spheric and deviatoric parts of the stress tensor, reduced to the cross section, are decoupled. To achieving this decoupling, Charmetant et al. [23] proposed a transverse isotropic hyperelastic fibrous model, which relies on four deformation modes represented in Figure 3:

(a) Elongation of the fibres
(b) Compaction, representative of fibre density in the cross section
(c) Distortion, representative of fibre rearrangement in the cross section
(d) Longitudinal shearing, representative of fibre sliding

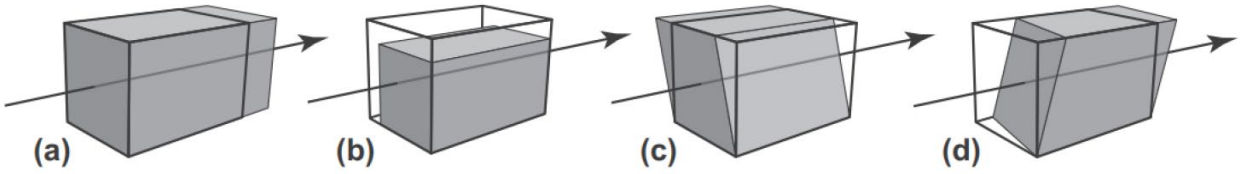

Fig.3°: Charmetant law modes, a) elongation, b) compaction, c) distortion, d) shearing.

Charmetant work was based on a special mode decomposition proposed by Criscione et al. [24] who defined, based on the assumption of transverse isotropy, an orthogonal frame in which the deformation gradient tensor F is written:

Materials Research Proceedings 41 (2024) 449-456 https://doi.org/10.21741/9781644903131-50

$$\left[\underline{\underline{F}}\right] = \begin{bmatrix} f_m & f_{m1} & f_{m1} \\ 0 & f_{11} & 0 \\ 0 & 0 & f_{22} \end{bmatrix}_{\left(\underline{M},\underline{N_1},\underline{N_2}\right)} \quad (5)$$

where $\underline{M}$ is the unitary vector that represents the preferred direction of the fibres, and ($\underline{N_1}$, $\underline{N_2}$) are two orthogonal unitary vectors, in the cross section, that stays orthogonal throughout the transformation. One of the Charmetant law innovation was to build a physically based set of invariants easily measurable experimentally. All of them are expressed from the deformation gradient tensor components (5):

$$I_{elong} = \ln(f_m) \; ; \; I_{comp} = \frac{1}{2}\ln(f_{11}f_{22}) \; ; \; I_{dist} = \frac{1}{2}\ln\left(\frac{f_{11}}{f_{22}}\right) \; ; \; I_{shear} = \sqrt{\frac{{f_{11}}^2+{f_{22}}^2}{{f_m}^2}} \quad (6)$$

Given the independency of each deformation mode, the energy potential is written as the sum of every single mode potential written as:

$$W_{elong} = \frac{1}{2}K_{elong}{I_{elong}}^2 \; ; \; W_{comp} = K_{comp}{I_{comp}}^p \; if \; I_{comp} \leq 0 \; or \; W_{comp} = 0 \; ;$$
$$W_{dist} = \frac{1}{2}K_{dist}{I_{dist}}^2 \; ; \; W_{shear} = \frac{1}{2}K_{cis}{I_{dist}}^2 \quad (7)$$

Fibrous Finite Element Formulation

The present formulation is based on various assumptions [14, 15]:

- Fictive fibres are considered all along the thickness of the element and they can be seen as unitary cross section Bernoulli beams sharing the same nodes as the element.
- Deformation modes are fully independent so they might not obey to the same material law and do not need to be integrated in the same way into the element.
- NEM are used [16, 17, 18].

In the case of the solid-beam element, fictive fibres are located at the edge of the hexahedral element and are aligned with the ξ direction corresponding to the anisotropic one, i.e. the fibre's direction, as represented in Figure 4. Therefore, the deformation modes occurring in the fibre direction (resp. cross section) are referred to as "longitudinal modes" (res. "transverse modes").

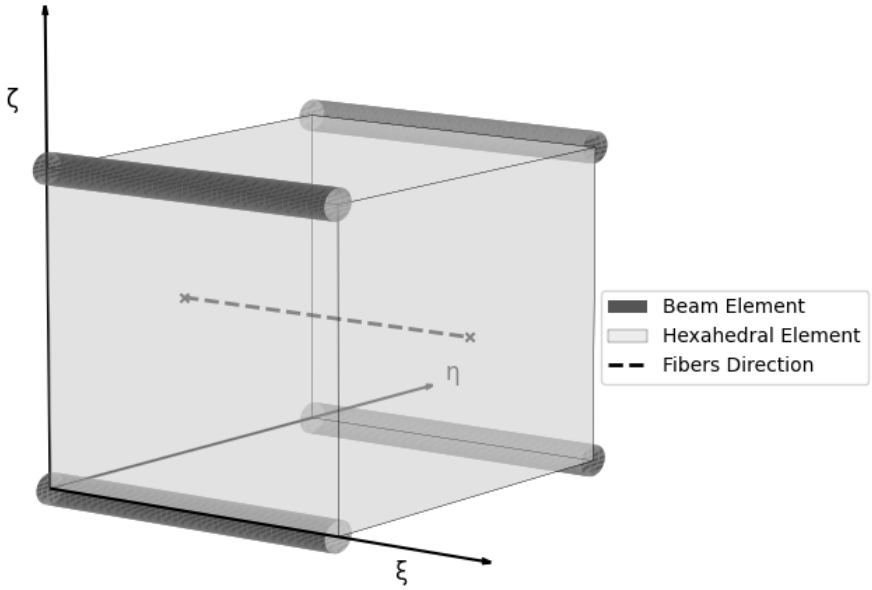

Fig.°4: Fibrous solid-beam element scheme in its reference configuration.

The tension behaviour is assumed to be linear elastic and will be integrated in a single Gauss point into the beam element. The same assumption is done for the bending behaviour, whose curvature will be calculated thanks to NEM at two Gauss points. The hexahedral element is a classical reduced integrated one with the transverse isotropic hyperelastic Charmetant law [23]. It handles the thickness behaviour of the yarn, which means compaction, transverse shear and longitudinal shear, illustrated in Figure 5.

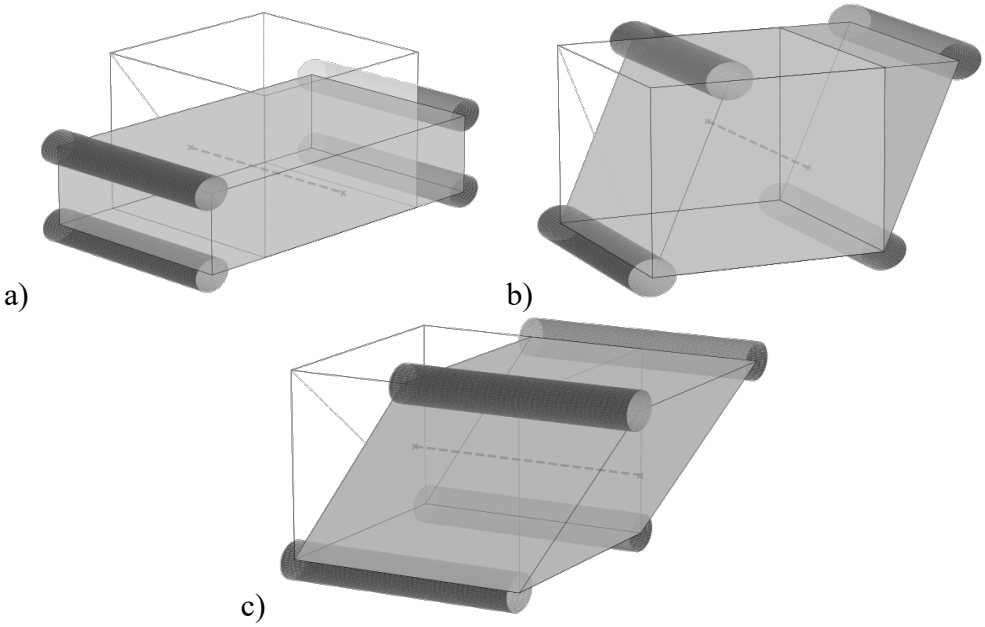

Fig.5°: Thickness behaviour deformation modes a) transverse compression, b) transverse shear, c) longitudinal shear.

Contrary to Charmetant law, tension deformation potential is considered null because superimposed beam elements already ensure this mode and the quasi-inextensibility of fibres. Consequently, since beams and hexahedral elements share the same nodes, longitudinal length will not extend when the element is compressed.

Numerical Analysis

The efficiency and accuracy of this fibrous solid-beam element has been tested throughout the simulation of a cantilever test and compared with an experiment performed with a set of several layers of Hexcel G986 reinforcement held together by soft threads [14]. The right tip of the sample is clamped and the rest is free and subjected to its own weight. This test is relevant for observing material normal orientation, drawn in white on Fig.6 (a), as it has been done by Boisse *et al.* [11] to show that neither Kirchhoff nor Reissner assumptions hold.

A qualitative comparison between experimental and numerical results has been performed based on kinematic considerations such as the orientations of material normal, the shape of the free tip and the thickness evolution along the longitudinal axis.

Boundary conditions of the numerical model are:

- Right tip nodes clamped.
- Left tip nodes vertical displacement imposed.

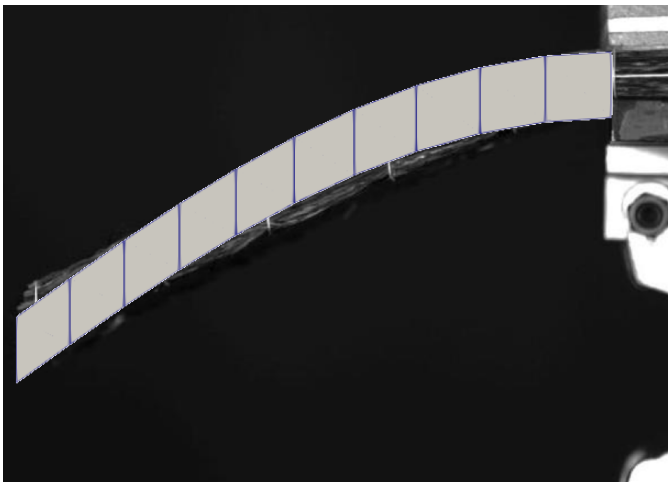

Fig.6°: Cantilever test on a multilayer reinforcement comparison between experiment and simulation

Since each layer is free to slide on its neighbours, the free tip of the sample has a bevel shape and the material normal stays vertical. Furthermore, the thickness of the sample doesn't change because the plies are held together and thus no delamination can appear. Thanks to this results, fibrous solid-beam element model will be able to properly simulate kinematic response of yarns.

Summary

A new solid-beam finite element formulation based on phenomenological observations on textile reinforcements is developed. It is a generalization of the fibrous element formulation for a mesoscopic modelling purpose. The neighbour element method is used to calculate curvature, which ensures that bending behaviour is fully independent of the other deformation modes. These modes are taken into account using Charmetant transverse isotropic hyperelastic law.

This element will be tested on mesoscopic models soon. A characterization campaign is also yet to be done to identify Charmetant law parameters.

References

[1] N. Naouar, E. Vidal-Sallé, J. Schneider, E. Maire, et P. Boisse, « Meso-scale FE analyses of textile composite reinforcement deformation based on X-ray computed tomography », *Composite Structures*, vol. 116, p. 165-176, sept. 2014. https://doi.org/10.1016/j.compstruct.2014.04.026

[2] G. Hivet et P. Boisse, « Consistent 3D geometrical model of fabric elementary cell. Application to a meshing preprocessor for 3D finite element analysis », *Finite Elements in Analysis and Design*, vol. 42, nº 1, p. 25-49, oct. 2005. https://doi.org/10.1016/j.finel.2005.05.001

[3] P. Badel, E. Vidal-Sallé, et P. Boisse, « Large deformation analysis of fibrous materials using rate constitutive equations », *Computers & Structures*, vol. 86, nº 11-12, p. 1164-1175, juin 2008. https://doi.org/10.1016/j.compstruc.2008.01.009

[4] R. Zheng, « A unit-cell mesoscale modelling of biaxial non-crimp-fabric based on a hyperelastic approach », Materials Research Proceedings 28, mai 2023, p. 285-292. doi: 10.21741/9781644902479-31

[5] Q. T. Nguyen *et al.*, « Mesoscopic scale analyses of textile composite reinforcement compaction », *Composites Part B: Engineering*, vol. 44, nº 1, p. 231-241, janv. 2013. https://doi.org/10.1016/j.compositesb.2012.05.028

[6] P. Boisse, N. Hamila, E. Vidal-Sallé, et F. Dumont, « Simulation of wrinkling during textile composite reinforcement forming. Influence of tensile, in-plane shear and bending stiffnesses », *Composites Science and Technology*, vol. 71, nº 5, p. 683-692, mars 2011. https://doi.org/10.1016/j.compscitech.2011.01.011

[7] B. Chen, J. Colmars, N. Naouar, et P. Boisse, « A hypoelastic stress resultant shell approach for simulations of textile composite reinforcement forming », *Composites Part A: Applied Science and Manufacturing*, vol. 149, p. 106558, oct. 2021. https://doi.org/10.1016/j.compositesa.2021.106558

[8] A. Iwata, T. Inoue, N. Naouar, P. Boisse, et S. V. Lomov, « Coupled meso-macro simulation of woven fabric local deformation during draping », *Composites Part A: Applied Science and Manufacturing*, vol. 118, p. 267-280, mars 2019. https://doi.org/10.1016/j.compositesa.2019.01.004

[9] J. Wang, P. Wang, N. Hamila, et P. Boisse, « Meso-Macro Simulations of the Forming of 3D Non-Crimp Woven Fabrics », *Textiles*, vol. 2, nº 1, p. 112-123, févr. 2022. https://doi.org/10.3390/textiles2010006

[10] S. Gatouillat, A. Bareggi, E. Vidal-Sallé, et P. Boisse, « Meso modelling for composite preform shaping – Simulation of the loss of cohesion of the woven fibre network », *Composites Part A: Applied Science and Manufacturing*, vol. 54, p. 135-144, nov. 2013. https://doi.org/10.1016/j.compositesa.2013.07.010

[11] P. Boisse, N. Hamila, et A. Madeo, « The difficulties in modeling the mechanical behaviour of textile composite reinforcements with standard continuum mechanics of Cauchy. Some possible remedies », *International Journal of Solids and Structures*, vol. 154, p. 55-65, déc. 2018. https://doi.org/10.1016/j.ijsolstr.2016.12.019

[12] P. Boisse, J. Colmars, N. Hamila, N. Naouar, et Q. Steer, « Bending and wrinkling of composite fibre preforms and prepregs. A review and new developments in the draping simulations », *Composites Part B: Engineering*, vol. 141, p. 234-249, mai 2018. https://doi.org/10.1016/j.compositesb.2017.12.061

[13] D. Dörr, F. J. Schirmaier, F. Henning, et L. Kärger, « A viscoelastic approach for modeling bending behaviour in finite element forming simulation of continuously fibre reinforced

composites », *Composites Part A: Applied Science and Manufacturing*, vol. 94, p. 113-123, mars 2017. https://doi.org/10.1016/j.compositesa.2016.11.027

[14] B. Liang, J. Colmars, et P. Boisse, « A shell formulation for fibrous reinforcement forming simulations », *Composites Part A: Applied Science and Manufacturing*, vol. 100, p. 81-96, sept. 2017. https://doi.org/10.1016/j.compositesa.2017.04.024

[15] R. Bai, J. Colmars, N. Naouar, et P. Boisse, « A specific 3D shell approach for textile composite reinforcements under large deformation », *Composites Part A: Applied Science and Manufacturing*, vol. 139, p. 106135, déc. 2020. https://doi.org/10.1016/j.compositesa.2020.106135

[16] M. Brunet et F. Sabourin, « A simplified triangular shell element with a necking criterion for 3-D sheet-forming analysis », *Journal of Materials Processing Technology*, vol. 50, nº 1-4, p. 238-251, mars 1995. https://doi.org/10.1016/0924-0136(94)01384-D

[17] F. Sabourin et M. Vives, « Eléments finis triangulaires pour la simulation de l'emboutissage: Aspects de base », *Revue Européenne des Éléments Finis*, vol. 10, nº 1, p. 7-53, janv. 2001. https://doi.org/10.1080/12506559.2001.11869238

[18] F. Sabourin et M.l Brunet,"Detailed formulation of the rotation-free triangular element "S3" for general purpose shell analysis", Engineering Computations, Vol. 23 Iss 5 pp. 469 – 502, juil 2006. https://doi.org/10.1108/02644400610671090

[19] T. Belytschko *et al*., « Non linear finite elements for continua and structures », first ed, John Wiley & Sons, 1998.

[20] E. De Bilbao, D. Soulat, G. Hivet, et A. Gasser, « Experimental Study of Bending Behaviour of Reinforcements », *Exp Mech*, vol. 50, nº 3, p. 333-351, mars 2010. https://doi.org/10.1007/s11340-009-9234-9

[21] T. Abdul Ghafour, J. Colmars, et P. Boisse, « The importance of taking into account behaviour irreversibilities when simulating the forming of textile composite reinforcements », *Composites Part A: Applied Science and Manufacturing*, vol. 127, p. 105641, déc. 2019. https://doi.org/10.1016/j.compositesa.2019.105641

[22] P. Badel, E. Vidal-Sallé, E. Maire, et P. Boisse, « Simulation and tomography analysis of textile composite reinforcement deformation at the mesoscopic scale », *Composites Science and Technology*, vol. 68, nº 12, p. 2433-2440, sept. 2008. https://doi.org/10.1016/j.compscitech.2008.04.038

[23] A. Charmetant, E. Vidal-Sallé, et P. Boisse, « Hyperelastic modelling for mesoscopic analyses of composite reinforcements », *Composites Science and Technology*, vol. 71, nº 14, p. 1623-1631, sept. 2011. https://doi.org/10.1016/j.compscitech.2011.07.004

[24] J. Huang, P. Boisse, N. Hamila, et Y. Zhu, « Simulation of Wrinkling during Bending of Composite Reinforcement Laminates », *Materials*, vol. 13, nº 10, p. 2374, mai 2020. https://doi.org/10.3390/ma13102374